BIOCYBERNETIC FACTORS IN HUMAN PERCEPTION AND MEMORY

David C. Lai

Stanford University

Prepared for:

Advanced Research Projects Agency

January 1975

SEL-75-001

SEMI-ANNUAL REPORT

for the Advanced Research Projects Agency

of the Department of Defense

BIOCYBERNETIC FACTORS IN HUMAN PERCEPTION AND MEMORY

PRINCIPAL INVESTIGATOR:

Dr. David C. Lai

Contract No. DAHC15-72-C-0232

ARPA Order No. 2190

January 1975

Technical Report No. 6741-4

1 June 1975 to 30 November 1974

Department of Electrical Engineering
Stanford Electronics Laboratories
Stanford University Stanford, California 94305

The views and conclusions contained in this document are those of the authors and should not be interpreted as necessarily representing the official policies, either expressed or implied, of the Advanced Research Projects Agency or the U. S. Government.

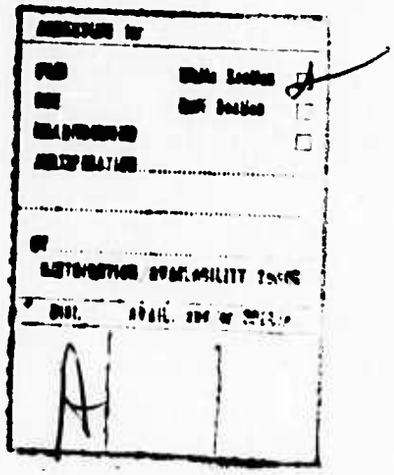

PROFESSIONAL PERSONNEL

Dr. D. C. Lai, Visiting Professor of Electrical Engineering, Principal Investigator

Dr. T. Kailath, Professor of Electrical Engineering, Co-Principal Investigator

Dr. H. S. Magnuksi, Post-doctoral Research Fellow

Dr. J. E. Anliker, Consultant

L. D. Stricklan (B.S.E.E.C.S.), Scientific Programmer

A. Huang (M.S.E.E.), Scientific Programmer

A. Shah (M.S.E.E.), Graduate Student Research Assistant

J. Nickolls (M.S.E.E.), Graduate Student Research Assistant

R. Floyd (M.S.E.E.), Graduate Student Research Assistant

FOREWORD

This semi-annual technical report presents the accomplishments of this project during the period of 1 June 1974 through 30 November 1974. Since the inception of this project, it has been the result of the collaborative efforts of many individuals. Most of the staff members contributed to the making of this report.

Biocybernetic Factors in Human Perception and Memory

SUMMARY

The goal of this research project is to develop biocybernetic concepts and techniques useful for the analysis and development of skills needed for the enhancement of concrete images of the "eidetic" type. We treat scanpaths of the eye during observation of visual patterns as indicators of the brain's strategy for the intake of visual information. We attempt to determine the features that differentiate visual scanpaths associated with superior imagery from scanpaths associated with inferior imagery, and simultaneously, to differentiate the electroencephalographic features correlated with superior imagery from those correlated with inferior imagery. Incorporating this information, we shall design and implement a closely-coupled man-machine system to generate image enhancement and to train the individual to exert greater voluntary control over his own imagery. Significant progress has been made in this reporting period.

We believe that the strategy of an individual with superior imagery is to fixate his eyes at optimal positions of the visual pattern at optimal time instants in relation to EEG. Our study of the visual scanpaths while viewing a stationary scene and the development of an EEG model is aimed at obtaining a firmer grip of these optimal locations and optimal time instants. We have also developed models for saccadic eye movement for the purpose of providing more accurate prediction of eye positions and tracking of eye movements. Some recent results are presented in this report and at various international and national scientific conferences.

The implications of this research project are signficant for the Department of Defense since the results obtained from this research will enhance the potential for devising new techniques that will permit the development of the required skills for stronger imagery in individuals with normal memories. Because it is an important asset for the military person to have the ability to absorb information rapidly, to retain it intact for long periods of time, and to recall it instantly when needed, in this project we strive to intensify the post-stimulus imagery as far as possible towards "eidetic" memory and to search out those features of successful retrieval strategies so as to strengthen the individual's redintegration power.

TABLE OF CONTENTS

LIST OF FIGURES

I. INTRODUCTION

The development and use of biocybernetic concepts and techniques for analyzing and developing skills essential for the enhancement of concrete images of the "eidetic" type are the major concerns of this project. Our effort has been concentrated on the problem of achieving biocybernetic expansion of visual memory by using a closely-coupled man-machine system which performs real-time monitoring, analysis, and feedback of spatial and temporal cues that play prominent roles in human memory encoding and retrieval. There exists strong evidence that the human nervous system depends upon these cues in memory encoding and recall, especially sensory images. The limited knowledge of human memory mechanisms has hampered our design of the closely-coupled man-machine system. We shall use this man-machine system for the measurement and prediction of human mnemonic performance as well as for the control and enhancement of mnemonic skills. Such a man-machine system for visual memory tracking and training was block diagramed in the previous technical report.

The main scheme is to develop and implement real-time techniques for monitoring and prediction of central nervous activities related to memory functions through the analysis and tracking of eye movements and EEG signals. The information thus gained in the analysis of the cortical activities will then be used to arrange extraordinary coninci-dences between eye pointing, cortical states, and the control of stimulus patterns by employing optimal control schemes. The visual stimuli are presented in various ways such as projection screen,

oscilloscopic displays, and GRAF/PEN system for dichopic or monopic viewing. By measuring eye positions, eye movements, and EEG signals we intend to obtain the optical and electrophysiological estimators useful for deciphering the cues that serve as keys to the encoding and recall of visual memory. Combining these techniques with various feedback schemes to close the control loop in our closely-coupled man-machine system, we are attempting to achieve tighter control over image persistence and image dissipation. In this man-machine system, we use computer-based models to predict; i.e., forward-time analysis, the kind of stimulus patterns which should be used in order to produce the desired future response. The eye-movement and EEG signal are the responses through which the cortical states are monitored. These responses are closely controlled since the models are designed to mimic the actual physiological processes as far as the stimulus-response relation is concerned. Significant progress has been made on the modeling of saccadic eye movements and EEG signals in the past half year. The closely-coupled man-machine system is being implemented on a PDP-15 computer. The necessary interface hardware and software have been designed and implemented by us. Our major task now is to close the feedback loop in this man-machine system. Accomplishments made towards this end will be described in this technical report.

Our effort has been concentrated on modeling of saccadic eye movements and EEG signals, and the determination of spatial cues that are keys to the encoding and retrieval of visual memory. In the next section, we shall describe methods for modeling and prediction of saccadic eye movements with the aim to obtain better eye-movement tracking. Preliminary results are very encouraging. In order to

differentiate the visual scanpaths associated with superior (eidetic) imagery from those associated with ordinary imagery, we need consistent means to characterize various scanpaths. We shall present the characterization of visual scanpaths by statistical means in Section III. It is essential to understand the relation between visual stimuli and the EEG signal for the determination of the temporal cues that are keys to the encoding and retrieval of visual memory. In Section IV, we describe a nonlinear oscillator to model the stimulus-response relationship. Many good results have been obtained from this model. The presentation of visual stimuli to the subjects is an ever-increasing task in this project. In Section V, we shall present a new flexible method (GRAF/PEN system) for generating visual stimulus patterns. In closing, we shall make concluding remarks and describe future works in the last section.

II. MODELING AND PREDICTION OF SACCADIC EYE MOVEMENTS

In order to implement the closely-coupled man-machine system for visual memory enhancement, it is important to study the saccadic movements of the eye and to be able to predict the target point of a saccade in the shortest time possible after its onset. This can help us in presenting visual cues at appropriate times and at the right locations in the visual field. To study and analyze simple saccades, we have designed the following experiment:

A moving target in the form of a plus (+) is presented on the CRT screen. The target starts at a fixed point F on one extreme of the screen and then moves horizontally to one of the six points T_i, $i = 1, \ldots, 6$, which are equidistant such that the extent of eye movements from F to T_i varies from 5° to 30°. From T_i, the target returns to F. The target remains stationary at each point for 1.5 seconds. In one run, the target goes through all of the six points. However, to avoid anticipation, the order is taken from a table of random permutations. Twenty-five such runs were made during one experiment. Thus, we have records of 25 saccades each of lengths from 5° to 30° (only saccades from F to T_i are considered). The eye movements are recorded on analog tape and later digitized. Using an algorithm based on the position and velocity of the eye movements, the start of the saccades is determined. For each length, the saccades are lined up at this starting point and averaged. In this way, we can determine the shape of a typical saccade. The position, velocity and acceleration for 10° and 15° saccades are shown in Figures 1 and 2. The vertical bars in the position and velocity curves represent the standard deviation

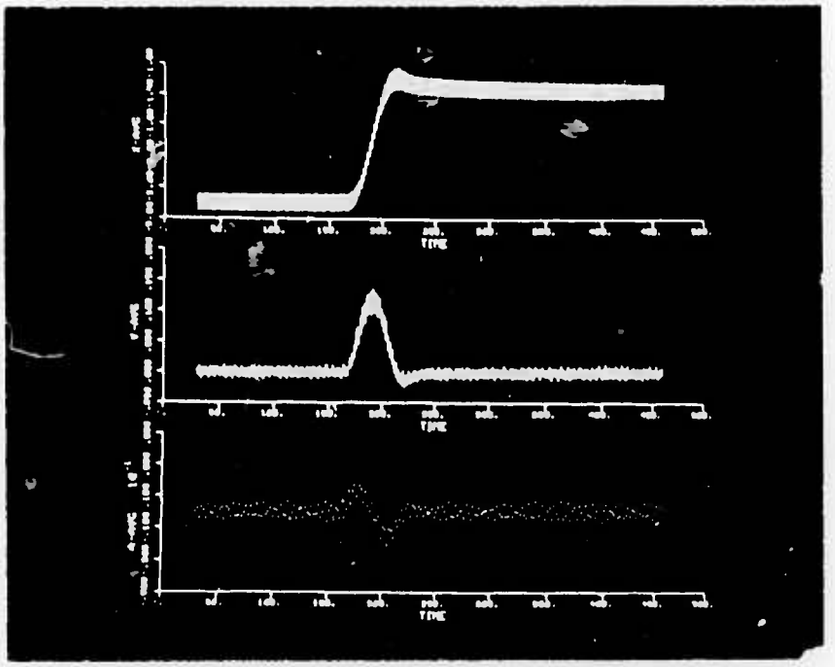

Figure 1 Averaged 10° saccade position, velocity, acceleration.

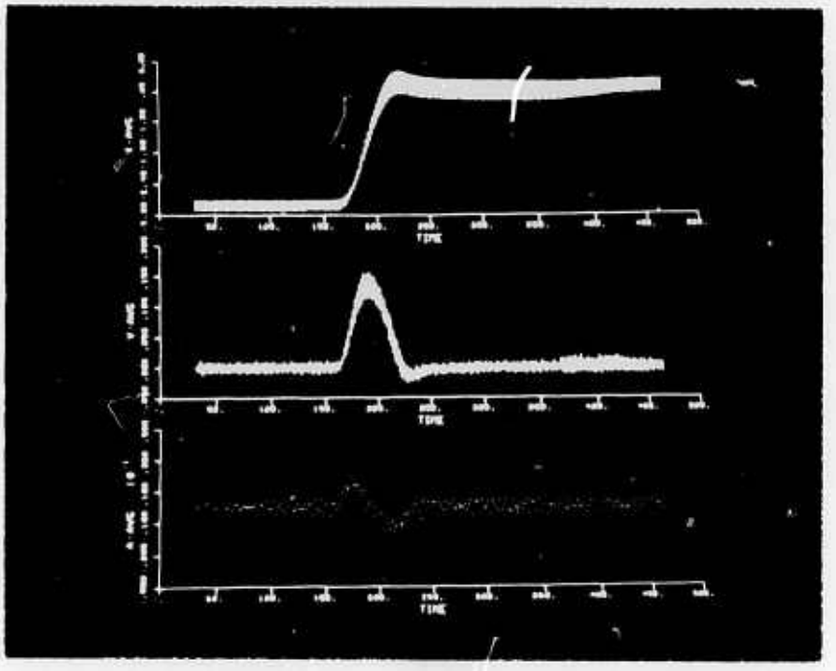

Figure 2 Averaged 15° saccade position, velocity, acceleration.

at each point.

The general shape of these curves agrees with that reported in the literature [1],[2],[3]. To model the curves or to use one of the existing models of the saccadic movement system [4],[5],[6] to fit the curves for prediction will be extremely useful for our purpose. We will attempt to fit a parametric functional equation to the saccade position curve. The relevant parameters have to be estimated. By extrapolation of this curve, we may then predict the endpoint of the saccade.

In particular, let us write

$$x_i = f\left(a_1, a_2, \ldots, a_k; t_k\right) + n_i$$

where x_i is the eye position at time t_i after the onset of the saccade, and $a_1, \ldots, a_k$ are the parameters which have to be estimated. n_i represents the noise term introduced by the measurement instrument, random nature of the biological system, human errors in taking data, etc. We assume that the system is stationary so that the characteristics of n_i can be determined from the eye movements during fixation when $f = 0$. Thus, the problem is two-fold: we first have to choose an appropriate function f and then to fit it to the saccade position curve in some optimum sense. We want to estimate the parameters a_i as soon after the onset of the saccade as possible. Prediction of the endpoint of the saccade can then be made.

We shall first assume that the functional form of the function f is known and shall consider only the problem of estimating the parameters. Our problem is to find $a_1, a_2, \ldots, a_k$ such that

$$S = \sum_i \left[x_i - f\left(a_1, a_2, \ldots, a_k; t_i\right)\right]^2$$

is minimized. They are the so-called least-squares estimates. These estimates coincide with the maximum likelihood estimates if n_i is white Gaussian noise. The least-squares estimates are quite easy to evaluate if f is linear in the a_i's. In such a case, the minimization problem reduces to solving a set of simultaneous linear equations.

The most natural linear functions to consider are polynomials. However, as can be seen from the averaged acceleration curves, the position curves have points of inflection, which a low order polynomial will not be able to achieve. Hence, we must look at other, possibly non-linear functions. Additional support for the nonlinearity of t comes from the existing models of the saccadic system. According to Robinson's model [5] of the plant shown below

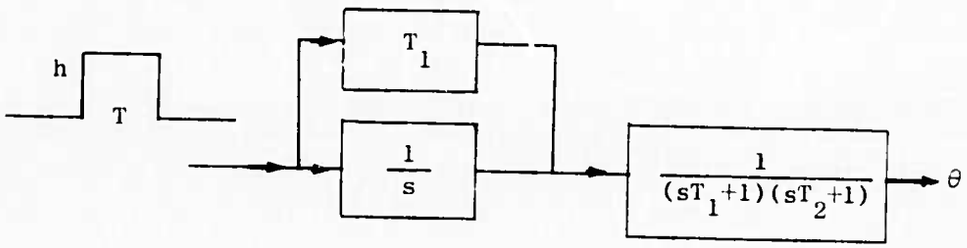

a saccade is produced by a pulse-step input to a second order system with transfer function

$$\left(T_1 + \frac{1}{s}\right) \frac{1}{(sT_1+1)(sT_2+1)} = \frac{1}{s(sT_2+1)}$$

The response of such a system to a pulse of height h and duration T is given by

$$\theta(t) = \begin{cases} hT_2\left[e^{-\frac{t}{T_2}} - 1 + \frac{t}{T_2}\right], & 0 \le t \le T \\ hT_2\left[e^{-\frac{t}{T_2}} - e^{-\frac{1}{T_2}(t-T)} + \frac{T}{T_2}\right], & t > T \end{cases}$$

From the above expression, we found that T is the time at which the velocity reaches a maximum. Thus, we can estimate the parameters h and T_2 from the position curve for $0 \le t \le T$. The saccade magnitude is hT so that we can predict it at this time.

In general, a nonlinear minimization problem can be solved by first linearizing the function by a Taylor series approximation about some initial estimates of the parameters and then solving the resulting set of linear equations and updating the parameters. This iteration is repeated until the desired accuracy is achieved.

$$x_i = f\left(a_1, a_2, \ldots, a_k; t_i\right) + n_i$$

$$= f\left(a_{10}, a_{20}, \ldots, a_{k0}; t_i\right) + \frac{\partial f}{\partial a_1} \Delta a_1 \Bigg|_{a_{10},\ldots a_{k0}, t_i} + \ldots + n_i$$

where $a_{10}, a_{20}, \ldots, a_{k0}$ are the initial estimates and $\Delta a_j = a_j - a_{j0}$. The first order partial derivatives of f are assumed to exist. They can be evaluated analytically or numerically.

Let

$$R_i = x_i - f\left(a_{10}, a_{20}, \ldots, a_{k0}; t_i\right)$$

Then

$$\min_{\Delta a_j} S = \sum_i \left(R_i - \frac{\partial f}{\partial a_1} \Delta a_1 - \frac{\partial f}{\partial a_2} \Delta a_2 \ \ldots \ - \frac{\partial f}{\partial a_k} \Delta a_k\right)^2$$

which now gives linear equations in Δa_j's. Solving these equations for Δa_j's, we can then update the a_{j0}'s. Since the above equation for $0 \le t \le T$ is nonlinear in only one parameter, a special method may be used. This method is described as follows:

Since

$$f(t) = \frac{h}{a}\left(e^{-at} - 1 + at\right) \qquad 0 \le t \le \tau \quad \text{where} \quad a = \frac{1}{T_2}$$

and

$$S = \sum_i \left[x_i - \frac{h}{a}\left(e^{-at_i} - 1 + at_i\right) \right]^2$$

Minimizing S with respect to h, we obtain

$$\frac{\partial S}{\partial h} = -2 \sum_i \left[x_i - \frac{h}{a}\left(e^{-at_i} - 1 + at_i\right) \right] \left(e^{-at_i} - at_i\right) \frac{1}{a} = 0$$

and thus

$$h = a \frac{\sum_i x_i \left(e^{-at_i} - 1 + at_i\right)}{\sum_i \left(e^{-at_i} - 1 + at_i\right)^2}$$

Setting

$$\frac{\partial S}{\partial a} = 0$$

to minimize S with respect to $\underline{a}$, and substituting the above expression for $\underline{h}$ in this equation, we can then solve for $\underline{a}$ by using zero-finding numerical techniques.

We have used this method for estimation of $\underline{h}$ and $\underline{a}$ for actual saccades from the experiment described before. The parameters are estimated by using the values of the eye position for $0 \le t \le T$ (where T is taken as the point of the velocity maxima). The parameters are then used for predicting the rest of the saccade curve. In Figures 3 and 4, we show the results in both parameter estimation and prediction of the saccadic movements for two different saccades. These preliminary results are encouraging.

One aspect of the saccade curve that this model cannot follow is

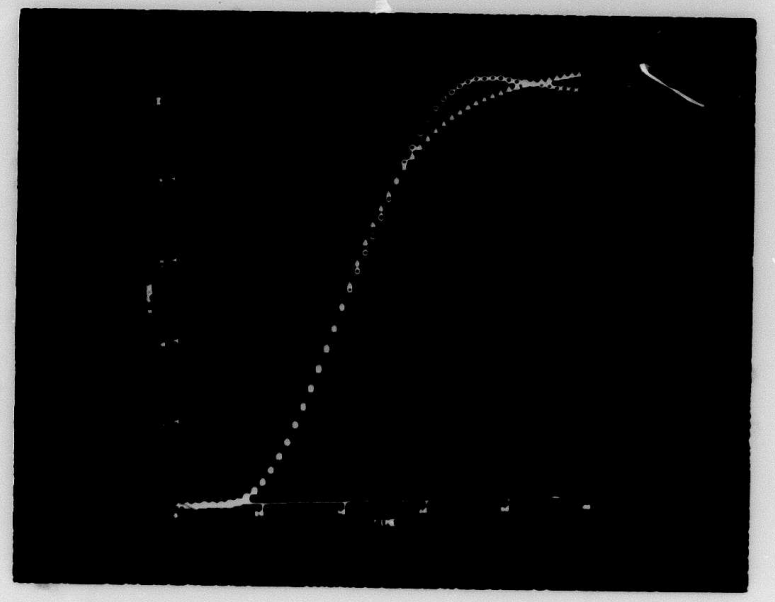

Figure 3 Estimation of parameters and prediction for a 20° saccade. Parameters estimated from first 43 ms (up to V_{max}) of data: a = .112 h = .237 ◯ - Actual curve - Predicted curve

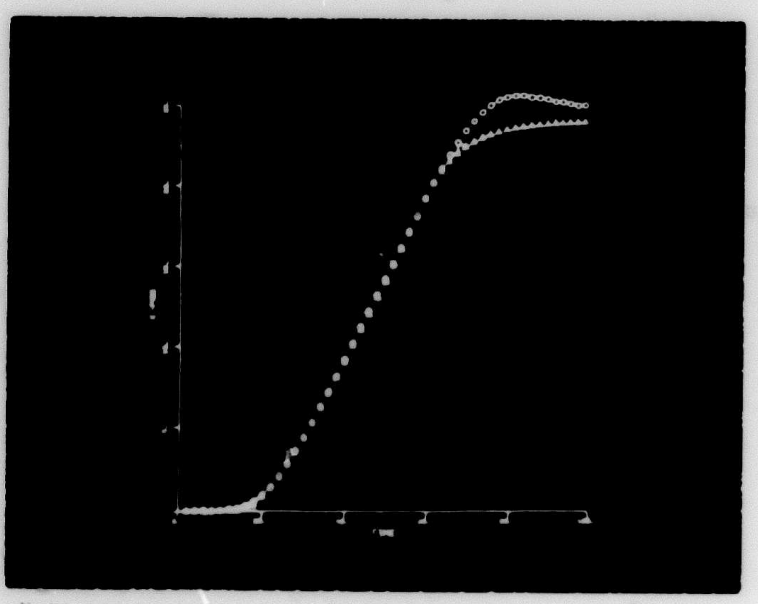

Figure 4 Estimation of parameters and prediction for a 25° saccade. Parameters estimated from first 60 ms (up to V_{max}) of data: a = .221 h = .180 ◯ - Actual curve - Predicted curve

the overshoot of the final position. The second order system is over-damped and hence overshoot will not occur. A remedy to this is to use the same plant model but with a different gain $T_3 \left(T_3 \neq T_1 \right)$ in the feed-forward path. Then the transfer function becomes

$$H(s) = \frac{(1+T_3 s)}{(1+T_1 s)(1+T_2 s)}$$

The response is now a sum of exponentials and by properly adjusting T_3 in relation to T_1, we can obtain the required overshoot. Work on this model is in progress.

III. CHARACTERIZATION OF SCANPATHS BY STATISTICAL MEANS

The measurement of performance of an observer in visual memory or visual search tasks is often a simple matter of scoring correct answers or monitoring the time taken to finish a given task. Assessing the reason why one observer does better than another is much more difficult, and involves an understanding of the strategy used by an observer to enhance his performance and an ability to describe the sequence of moves used to obtain the desired goal. In visual tasks the sequence of fixations used in scanning the visual target is called the scanpath, which has been shown to be an important component of an observer's performance [3],[7],[8]. Thus, there is a need to be able to characterize the scanpath, that is, to be able to describe features of it in terms other than a list of (X,Y) fixation coordinates.

One observation which has often been made is that the fixation points tend to be grouped around certain features or areas of the visual image, and are relatively sparse elsewhere. Thus, we can measure the nearness of one fixation point to another and assign a similarity measure to the two points based upon this distance. The ability to group or cluster a set of fixation points is an important step in the characterization of a scanpath, and several different techniques have been used to measure point similarities and to assign points to clusters.

A simple but useful measure of point similarity is based on the distance (d_{12}) in degrees between fixation points p_1 and p_2.

$$S_p\ (p_1, p_2) = e^{-d_{12}/d_f}$$

where S_p is the point similarity measure and d_f is a distance-decay

constant which can be chosen so that the similarity decreases at a rate approximately equal to the decrease in visual acuity as a function of distance from the center of the fovea. Typical values for d_f are 4 or 5 degrees.

An extension of the point similarity measure leads to a saccade similarity measure. Let the two saccades to be compared s_a and s_b have starting and ending point p_{1a}, p_{2a}, and p_{1b}, p_{2b}. Define

$$S_s\left(s_a, s_b\right) = S_p\left(p_{1a}, p_{1b}\right) \cdot S_p\left(p_{2a}, p_{2b}\right)$$

that is, the saccade similarity is the product of the similarity between starting and ending points of the saccades. This measure has certain properties that make it very suitable for comparing two saccades:

- S_s for identical saccades is one.
- S_s for very different saccades is near zero.
- As the difference between two saccdes increases, the similarity measure drops from one and approaches zero.
- S_s is sensitive to the direction of the saccadic jump.
- Unlike a vector dot product, absolute position is relevant.

We have used this saccade similarity measure on scanpath data consisting of several scans of a given scene by an observer. The saccades were compared pairwise and only those pairs of saccades with similarities greater than a certain threshold were retained. The resulting plot of saccades (Figure 5) clearly showed those transitions which were most likely and which occurred often. Thus, the saccade similarity measure is a simple and effective mechansim for determining the most frequently traversed paths followed by the eyes in viewing a picture.

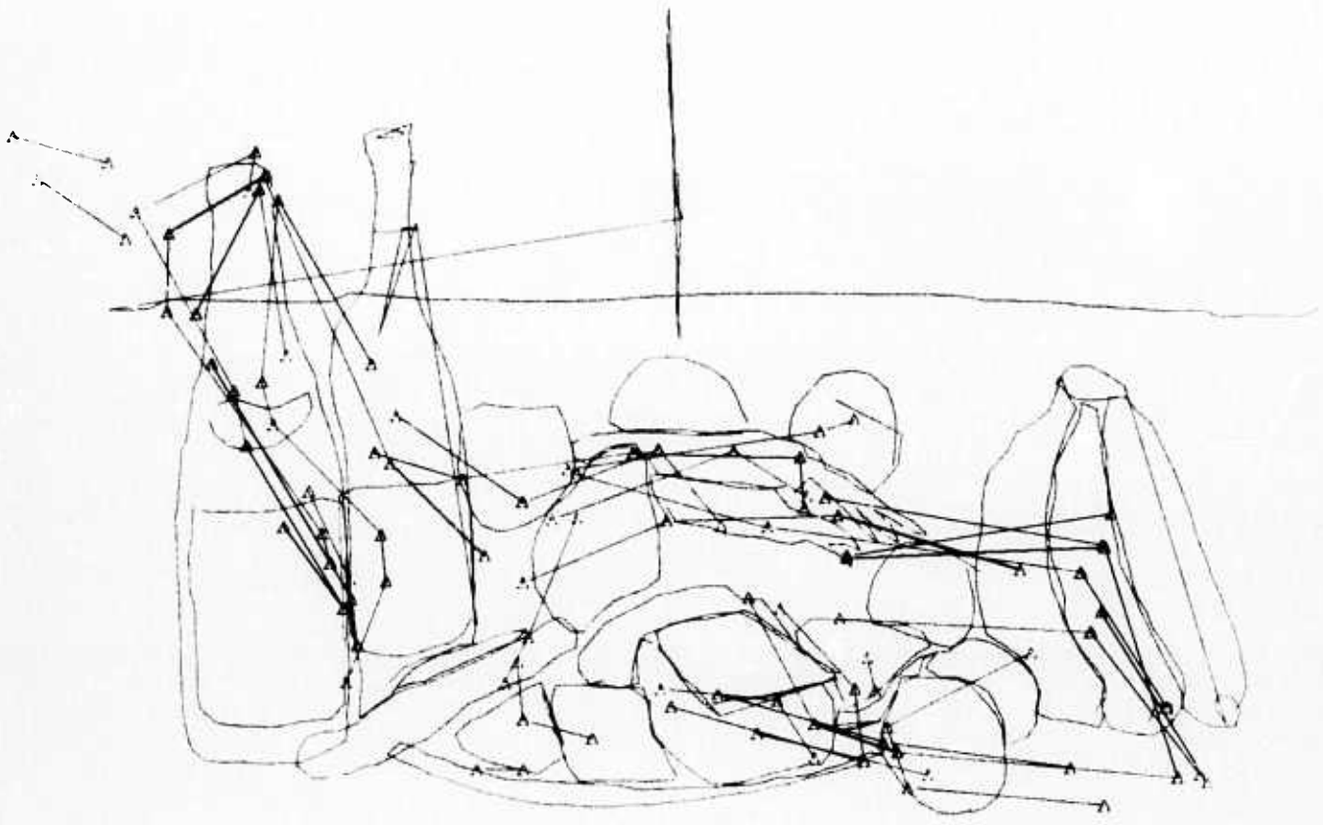

Figure 5 Outline drawing of still life scene viewed by an observer with most-similar saccades superimposed.

In addition to the above use of the similarity functions, we have developed an automatic method for determining if a given scanpath is cyclical or repeating in nature. By systematically comparing each saccade in a scan with its nearest neighbor, then next-nearest neighbor, and so on, and summing the similarity measures at each displacement, we compute an "autosimilarity" function of saccades which is very much like an autocorrelation function for a time series. Any cyclical componenets in the scan will appear as peaks in the autosimilarity function. The distance between peaks indicates the period (number of saccades) of the cycle. Figure 6 is a graph of the autosimilarity function for a scan having a pronounced cyclical tendency. In the same way, it is possible to derive a cross-similarity function for two different scans.

There exists an alternative approach to characterizing scanpaths, and it is based on the following two assumptions:

(a) There are a discrete number of "fixation centers" in the scene being viewed and each fixation point in the scan can be assigned to one of the fixation centers. This process of assignment is often called "clustering". The center of the clusters should be in close agreement with the centers of fixation. Due to the random nature of the fixation points, in any repetition (cycle) of the scanpath, the fixation points do not always coincide.

(b) A scanpath then becomes a sequence of transitions from one cluster center to another. Any saccade with starting and ending points in the same cluster is discarded.

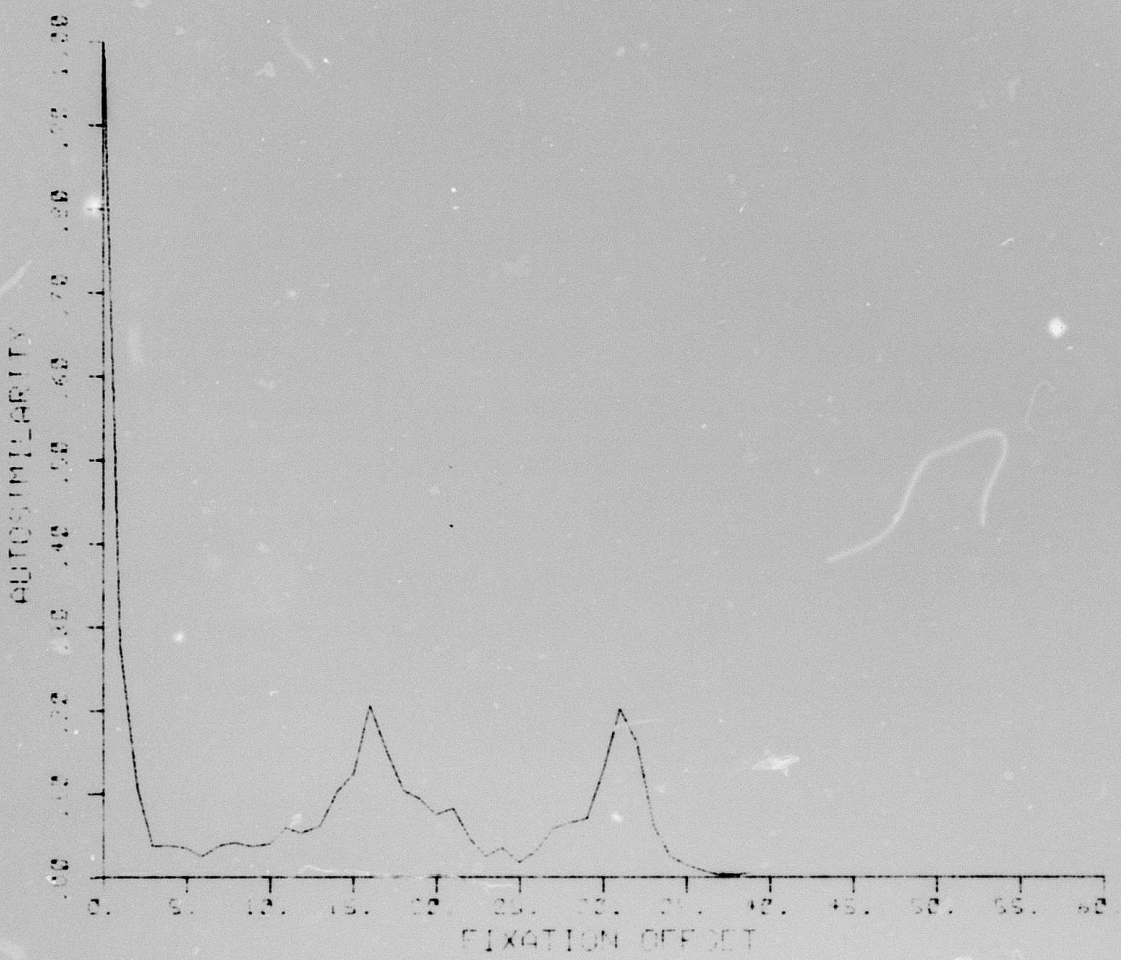

Figure 6 Autosimilarity plot for a single scanpath. Peaks indicate cyclical property of the scanpath. The distance between peaks is the number of saccades in the cycle.

From the set of all saccades leaving a given cluster center we can find the transition or transitions which have the highest probability. These transitions are termed the "most-probable-saccades". The "most-probable-scanpath" is then defined to be the set of all most-probable-saccades. The most-probable-scanpath depends on how the clusters are chosen, and is not necessarily a closed path through the cluster centers. Its usefulness is that it concisely summarizes the most important aspects of the scanpath used by the observer in viewing the given visual target.

We have used two different algorithms for selecting cluster centers, each with its own particular advantages and disadvantages. These algorithms are known as "ISODATA" and "Minimum-Spanning-Tree-Clustering" or MSTC.

In the ISODATA method [9] the number of clusters desired is given as an input variable, and the algorithm partitions the fixation points into subsets such that the total distance between the fixation points in a cluster and the cluster center is minimized for all clusters. The cluster center starting points are usually selected randomly, and the algorithm keeps moving the cluster centers until the above criterion has been reached.

The MSTC algorithm [10] automatically determines the number of clusters in the data and assigns fixation points to the clusters. Three variables given as input may be adjusted to change the criteria by which clusters are selected.

The chief advantages or disadvantages of these two algorithms are summarized below:

ISODATA

(1) Requires the desired number of clusters, which usually is not known.

(2) Solutions often are not unique, but vary with starting conditions.

(3) The iterations can require a substantial amount of computing.

(4) Many points can be easily accommodated.

MSTC

(1) The solution is unique, and the number of clusters is automatically determined.

(2) The computation is quite fast.

(3) Many points requires a large amount of storage.

Figures 7 and 8 illustrate how the second of these algorithms (MSTC) may be employed to reduce scanpath data to a more concise form. Figure 7 is a graph of a scanpath superimposed upon a line drawing representing the still life scene which the observer was viewing. The first recorded fixation (1) is in the center of the picture to the right of the label of the righthand wine bottle. The last fixation (70) is in the lower righthand position of the picture. The viewing time required to create this scan totaled 20 seconds. Figure 8 represents the same data after processing by the MSTC program. The program partitioned the fixation points into 23 subsets or clusters (using certain criteria supplied by the programmer) and then computed the most likely transitions from cluster to cluster. Clusters containing only one fixation point were ignored. The resulting plot shows the most likely saccades between areas containing large numbers of fixations, and presents the original data in a highly condensed format. These preliminary results are very promising. Refinements of this method are in progress.

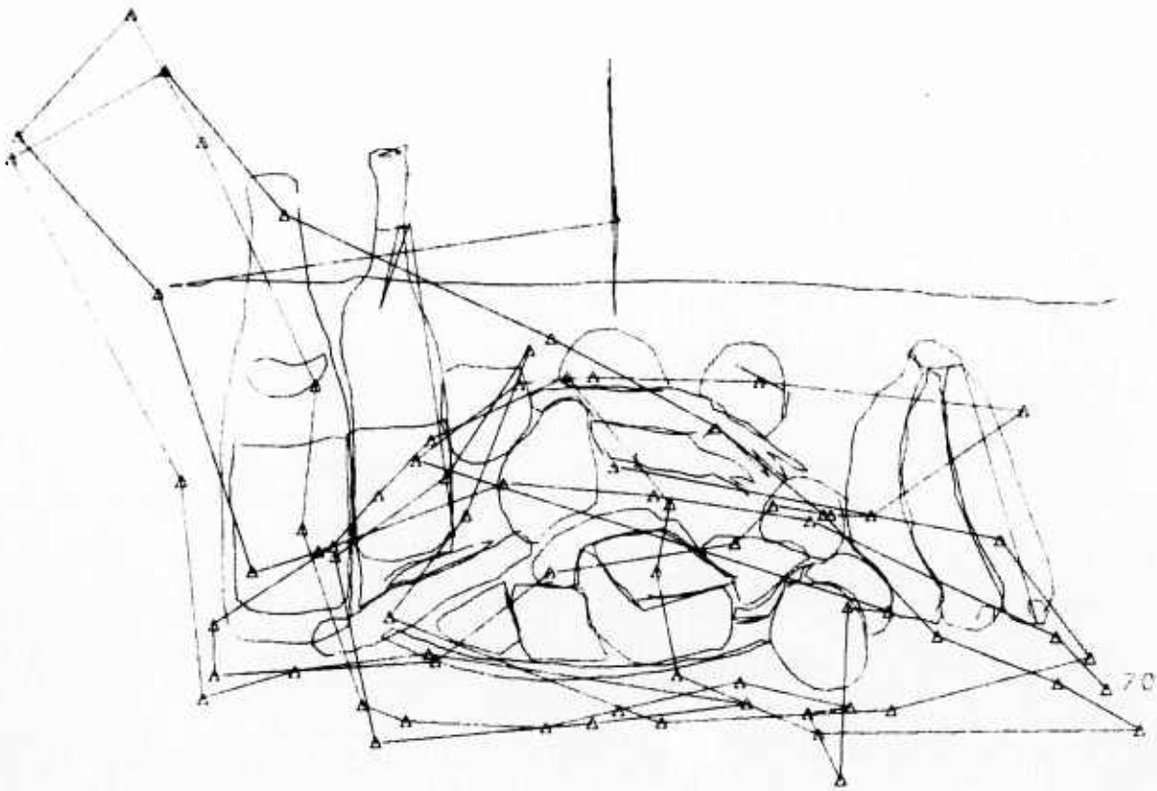

Figure 7 Scan of still life scene

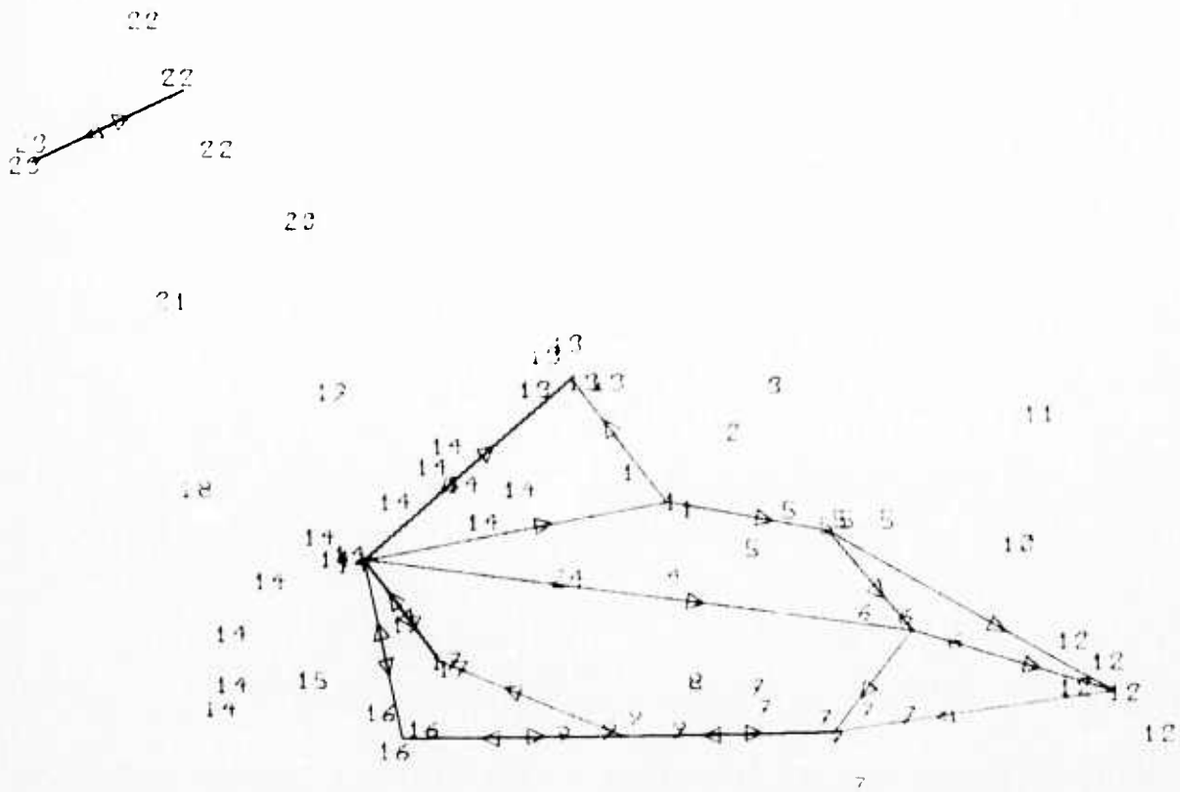

Figure 8 Most probable transitions between cluster centers.

IV. MODELING OF EEG SIGNALS DURING PERIODIC PHOTIC STIMULATION

1. Introduction

To better understand the relation between visual stimuli and the EEG signal, we have used a nonlinear oscillator to model the stimulus-response relationship. In particular, we are studying the entrainment of the alpha rhythm by periodic photic stimuli. This will enhance our understanding of the effect on EEG signals exerted by the repetitive photic stimulation and the various degrees of efficiency of the stimulus falling on various phases of the EEG signal. There is every reason to believe, based on the results of other researchers, that the eye takes in information only when it is fixating. One of our goals is to guide the eye to fixate only at those instances corresponding to the EEG phases while the brain is in the best state for processing information. We believe that there are relations between the effective phases for stimulation and the optimal phases for fixations. It is hoped that the development of a model for the entrainment process will elucidate the behavior of the alpha frequency and phase, and thus lead to a more practical brain state estimator and predictor in our memory studies.

Significant results have been obtained from the nonlinear oscillator model. A time-domain method of analysis for a pulse-train driven van der Pol oscillator was developed, and the resulting predictions were supported by new EEG data collected from several subjects. We will present the analysis along with model-generated results from a digital computer and compare with EEG results from human subjects.

2. A Nonlinear Mathematical Model for Entrainment of EEG Signals by Periodic Photic Stimulation

The model is a van der Pol oscillator representing the behavior of a subject's EEG during periodic stimulation by a stroboscope. The flashes are delivered for 20 seconds at some fixed frequency, followed by a 20 second stimulus-off period. This sequence is repeated for each desired stimulus frequency.

The van der Pol oscillator can be represented by

$$\ddot{x} - \mu\left(1 - x^2\right)\dot{x} + \omega_0^2 x = \omega_0^2 E(t)$$

where $x(t)$ denotes the EEG signal; ω_0 is the unstimulated alpha frequency; $E(t)$ is the external excitation (stimulus); and μ is the nonlinear coupling coefficient.

A first approximation to the solution $x(t)$ is readily made when $E(t)$ is a sinusoid, as discussed in the previous report, and the results in fact predict quite well our experimental data. However, since the experimental stimulus is a train of flashes, we have developed an analysis technique for approximating the solution of the van der Pol equation when $E(t)$ is a pulse train.

We assume that the unperturbed oscillation ($E(t) = 0$) is correctly represented by

$$x(t) = a_0 \sin \theta(t)$$

where the angular displacement can be written in terms of frequency and phase:

$$\theta(t) = \omega_0 t + \phi$$

We wish to examine the result of $E(t)$ being a series of impulses of strength q at a frequency ω_1.

Following a method due to Blacquière, we can assess the perturbation caused by one impluse. At an angular displacement

$$\vartheta_n = \omega_0 t_n + \phi$$

we apply the nth impulse. Its effect will be seen directly in $\dot{x}(t)$, causing a small step change $\Delta\dot{x} = q\omega_0^2$ over time Δt. However, x will be continuous, so $\Delta x = 0$.

To a first approximation, we can expand $\Delta\dot{x}$ and Δx as below:

$$\Delta x = \Delta a \sin \vartheta_n + a_0 \Delta\phi \cos \vartheta_n = 0$$

$$\Delta\dot{x} = \Delta a \omega_0 \cos \vartheta_n - a_0 \omega_0 \Delta\phi \sin \vartheta_n = q\omega_0^2$$

where Δa represents the change in amplitude and $\Delta\phi$ represents the change in phase of the system. Solving simultaneously for Δa and $\Delta\phi$, we obtain

$$\Delta a = q\omega_0 \cos \vartheta_n$$

$$\Delta\phi = -\frac{q\omega_0}{a_0} \sin \vartheta_n \quad .$$

In Figure 9, we demonstrate the amplitude and phase perturbations as a result of an impulse falling on angular displacement ϑ_n.

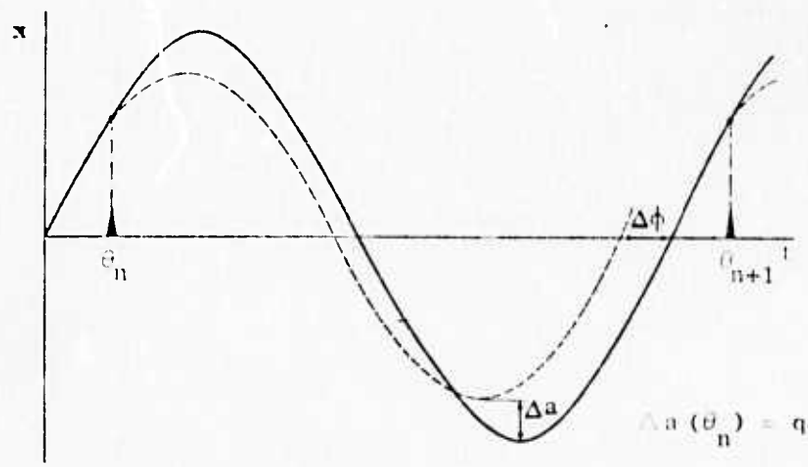

$$\Delta a(\vartheta_n) = q\omega_0 \cos \vartheta_n$$

$$\Delta\phi(\vartheta_n) = -\frac{q\omega_0}{a_0} \sin \vartheta_n$$

Figure 9 Phase and Amplitude Perturbations

The unperturbed solution would have followed the dashed line, and the perturbed solution follows the solid line.

In order to deal with a series of these impulses, Δa will be assumed to be negligible. This is reasonable since a more detailed analysis shows that the amplitude change decays exponentially with time. Let

$$T_0 = \frac{2\pi}{\omega_0}$$

$$T_1 = \frac{2\pi}{\omega_1}$$

be the alpha and stimulus periods, respectively. Then referring again to Figure 9, we see that applying the nth pulse at displacement θ_n results in a new displacement $\theta_n + \Delta\phi\left(\theta_n\right)$. Since the pulses are spaced T_1 seconds apart, the (n+1)th pulse will arrive at displacement

$$\theta_{n+1} = \theta_n + \Delta\phi\left(\theta_n\right) + T_1 \quad .$$

Clearly, for entrainment to occur, we must have

$$\left[\theta_{n+1}\right]_{\text{mod } T_0} = \left[\theta_n\right]_{\text{mod } T_0}$$

or

$$\left[\theta_n + \Delta\phi\left(\theta_n\right) + T_1\right]_{\text{mod } T_0} = \left[\theta_n\right]_{\text{mod } T_0} \quad .$$

Hence

$$\Delta\phi\left(\theta_n\right) + T_1 = k\, T_0 \quad , \; k = 0,\ 1,\ 2,\ \ldots \quad .$$

When $k = 0$, we have the unlikely situation of resetting the phase of oscillation; the required phase change $\Delta\phi\left(\theta_n\right)$ is very large. We will not consider this case here.

For $k = 1$, the solution is called harmonic entrainment, and for $k \geq 2$, it is called k^{th}-order superharmonic entrainment, where k represents the number of alpha periods elapsed per stimulus impluse. It is easy to show that this is stable near

$$\left[\theta_n\right]_{\text{mod } T_0} = 0 ,$$

as one would expect from the form of $\Delta\phi$.

In a similar fashion, for subharmonic entrainment to occur,

$$\left[\theta_{n+m}\right]_{\text{mod } T_0} = \left[\theta_n\right]_{\text{mod } T_0}$$

or

$$\left[\theta_n + \sum_{i=n}^{n+m-1} \Delta\phi\left(\theta_i\right) + m\, T_1\right]_{\text{mod } T_0} = \left[\theta_n\right]_{\text{mod } T_0} .$$

Hence,

$$\sum_{i=n}^{n+m-1} \Delta\phi\left(\theta_i\right) + m\, T_1 = T_0 .$$

When $m = 1$ we have harmonic entrainment again, and for $m \geq 2$, m^{th}-order subharmonic entrainment occurs. The stability of this solution is currently being investigated, but it appears that for $m = 2$ a small stable range exists.

In summary, when the stimulus frequency is near the alpha frequency, harmonic entrainment is possible. When the alpha frequency is near an integer multiple of the stimulus frequency, superharmonic entrainment is possible. And when the stimulus frequency is near an integer multiple of the alpha frequency, subharmonic entrainment is possible.

When the stimulus frequency is not in one of the above ranges, combined frequency oscillations exist. This can be easily seen by considering the spectrum of a sinusoid with perturbations at some other frequency. The

spectrum will have components at the stimulus frequency and its integer harmonics in addition to the autonomous component. We also expect similar harmonics to be present during the existence of entrainment. Results obtained from EEG data and the model are described and compared in the next section.

3. Theoretical Predictions and Comparison of Results

In Figure 10 an entire experimental record is presented. Each curve represents an integrated spectrum of the EEG taken over the entire 20-second stimulus-on period. A new stimulus frequency is used for each stimulus-on period. The horizontal axis is in hertz for all the spectrals, and the vertical axis may be considered to be the stimulus frequency as it is varied throughout the experiment. Starting from the bottom, the stimulus starts at 10 Hz., drops to .5 Hz., rises to 20 Hz., then drops back to 10 Hz. at the top. The stimulus frequency is changed by .5 Hz. for each new spectral. The five effects predicted in the previous section are visible in Figure 10: harmonic entrainment, superharmonic entrainment, subharmonic entrainment, combined frequency oscillations, and stimulus harmonics.

The van der Pol model has been simulated on a PDP-15 computer as described in the previous report. We will present some direct comparisons between the EEG spectra and the spectra generated by the model. The straight-line spectra are the model-generated predictions, and the smooth-curve spectra are EEG results taken from the record in Figure 10.

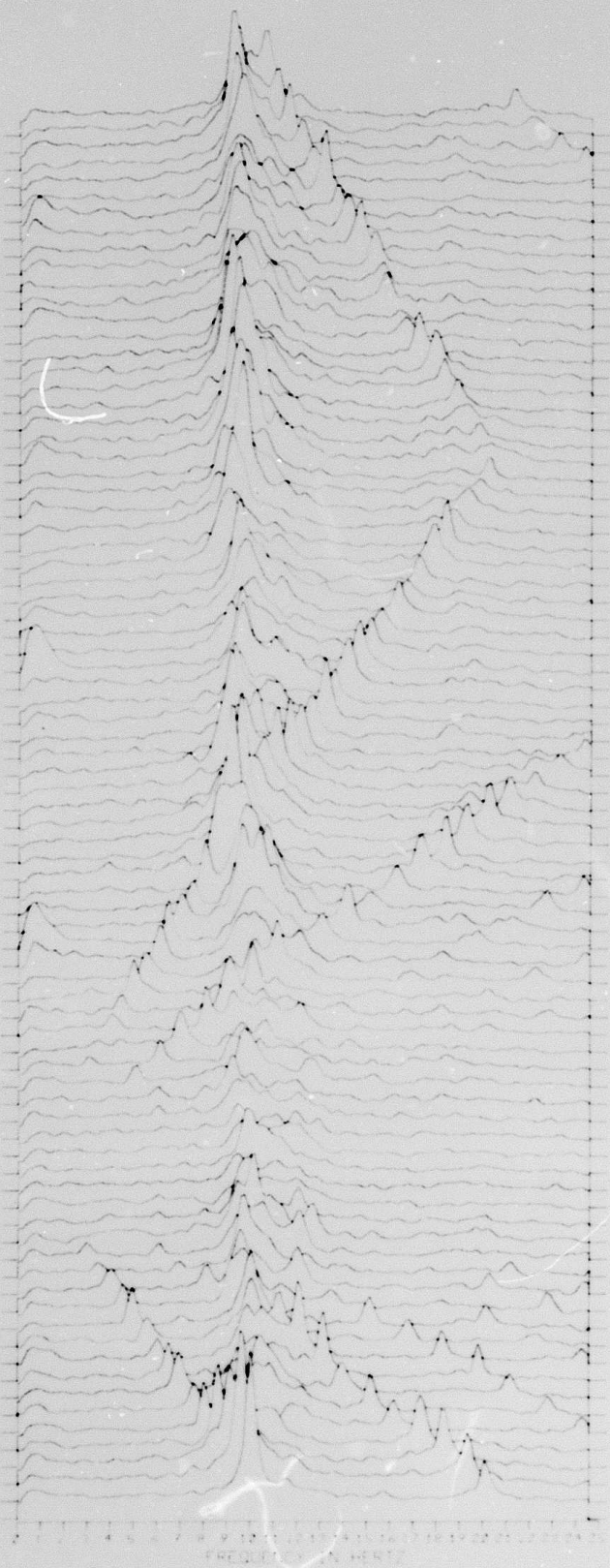

Figure 10 EEG spectra as a function of stimulus frequency.

Figure 11 shows the situation with no stimulus applied; $\omega_0/2\pi$ is adjusted to 9.7 Hz., the subject's alpha frequency. Figure 12 shows harmonic entrainment very close to the alpha frequency; note the harmonics. Harmonic entrainment is again seen in Figure 13. In Figure 14, second-order superharmonic entrainment can be seen; the alpha rhythm has shifted to twice the stimulus frequency. Figure 15 shows second-order subharmonic entrainment. This particular simulation is quite unstable (as expected) and is currently being investigated. Combined frequency oscillations can be seen in Figures 16, 17, and 18. Note the high-order stimulus harmonics in Figure 18. In Figure 19, we see that the stimulus occurs so infrequently that there is no discernible effect on the EEG spectrum, as one would predict from the previous analysis.

The experimental data exhibit the major frequency domain phenomena predicted by the model; we believe this is a significant step toward the understanding of some aspects of the alpha rhythm in EEG. Work is currently in progress to improve the model simulation, and investigations into the time-domain predictions of the model have been initiated. The analysis of the model in a previous section suggests the existence of some rather interesting EEG phase phenomena, which we feel will have direct bearing on the timing of eye fixation. It is anticipated that this nonlinear model will provide a good basis for prediction of cortical states needed for our memory studies.

Figure 11
EEG and simulated spectra in the
absence of stimulation

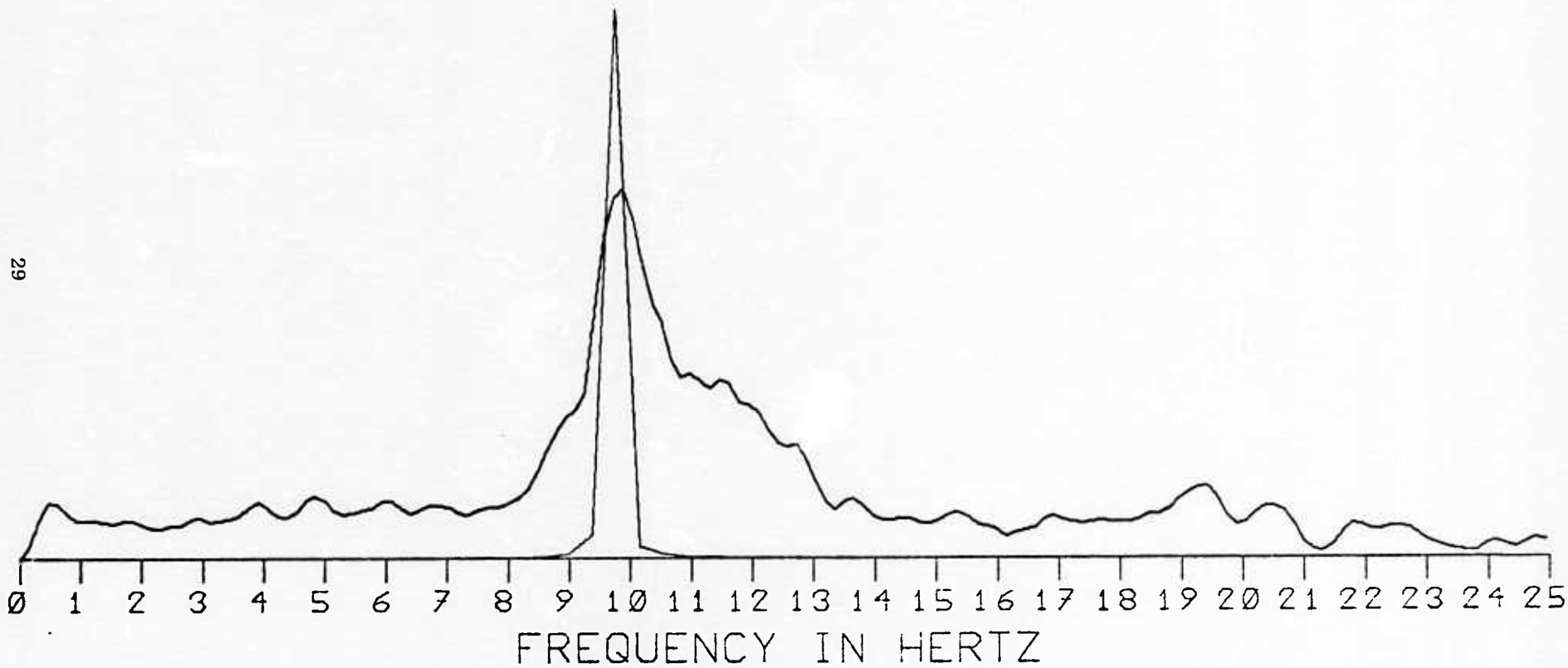

Figure 12
EEG and simulated spectra during
9.5 Hz. stimulation.

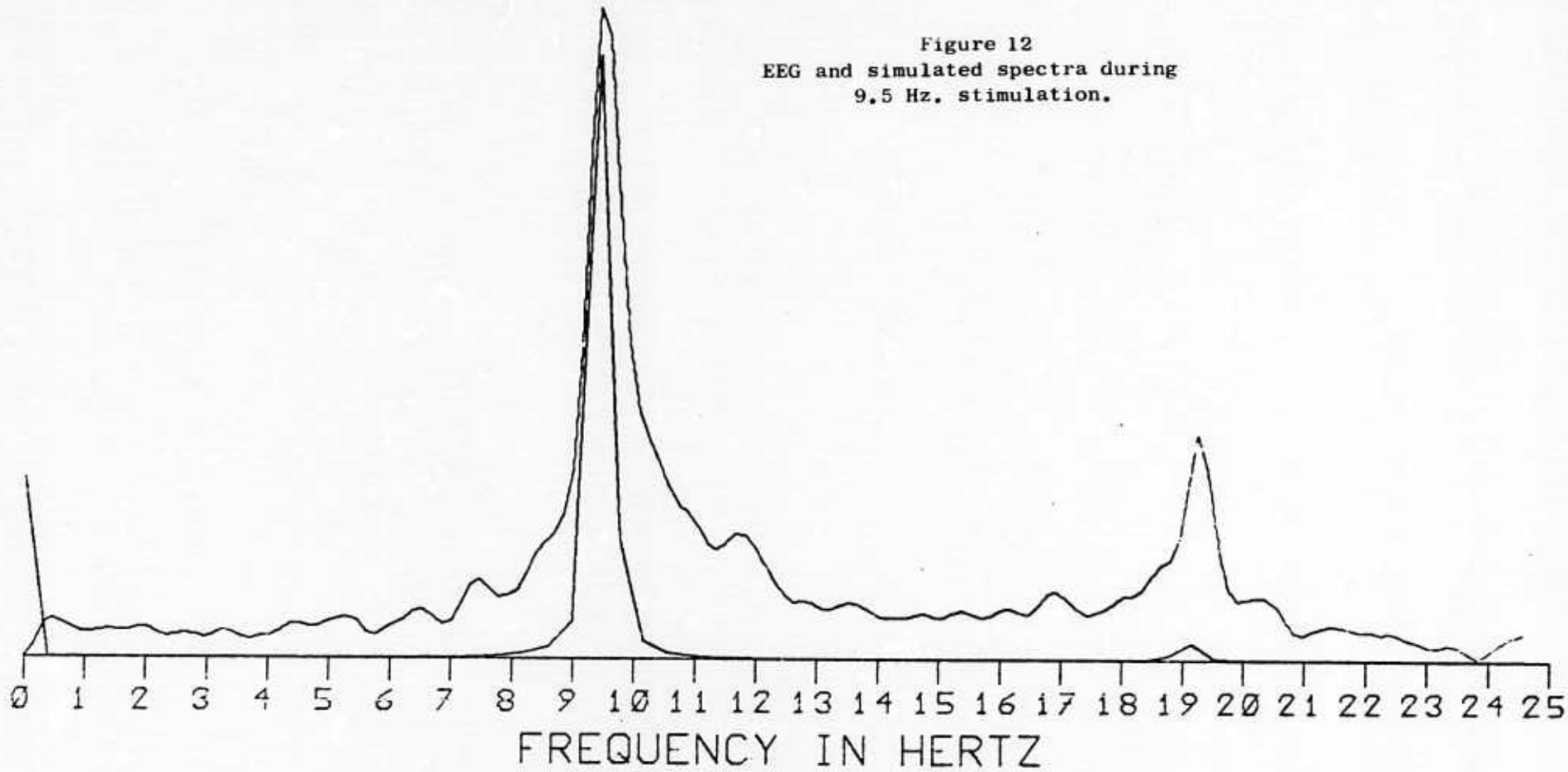

STIMULUS FREQUENCY = 9.50
COUPLING COEFFICIENT = .20000

Figure 13
EEG and simulated spectra during
10.0 Hz. stimulation.

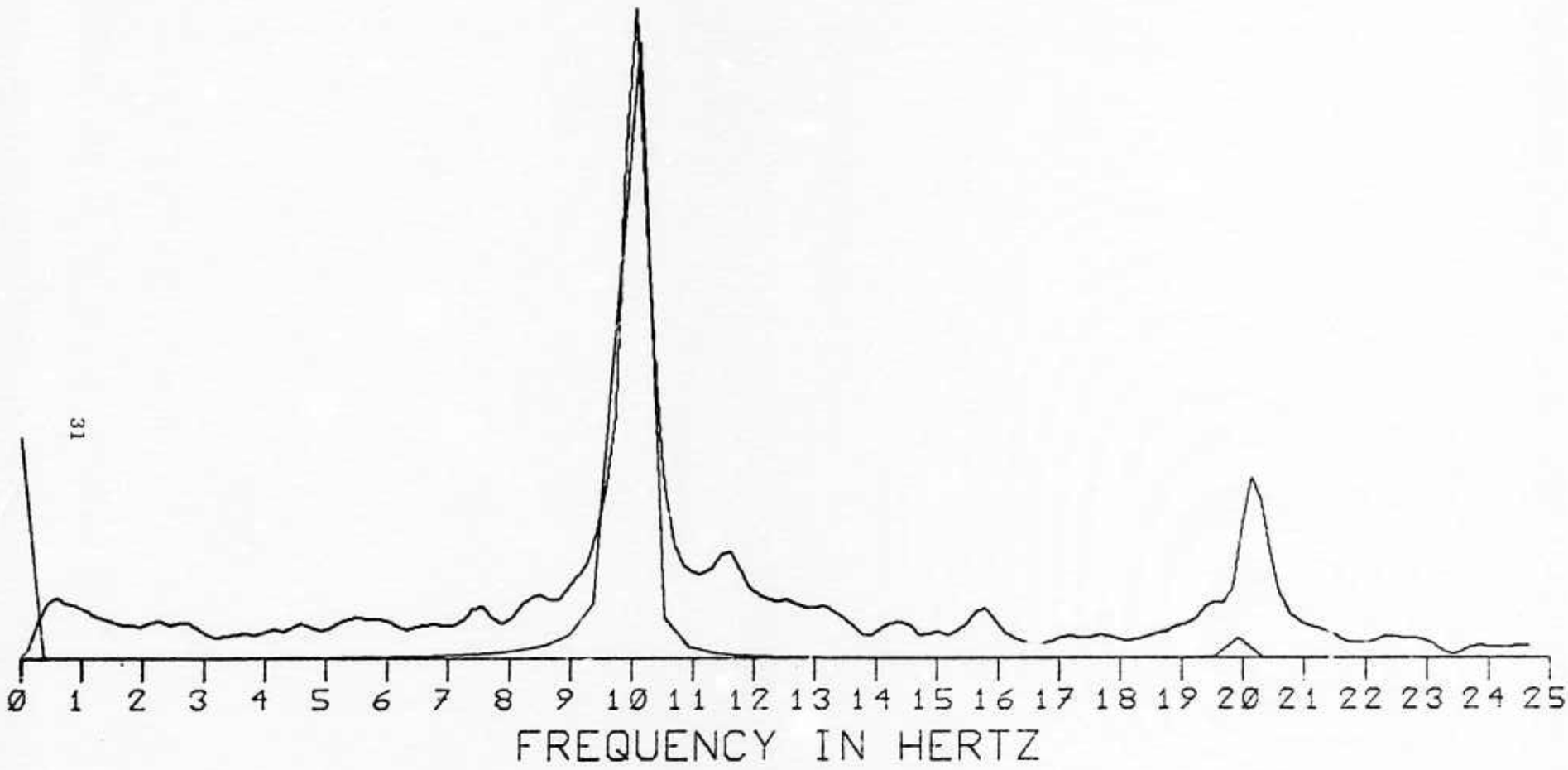

STIMULUS FREQUENCY = 10.00

COUPLING COEFFICIENT = .20000

Figure 14
EEG and simulated spectra during
5.0 Hz. stimulation.

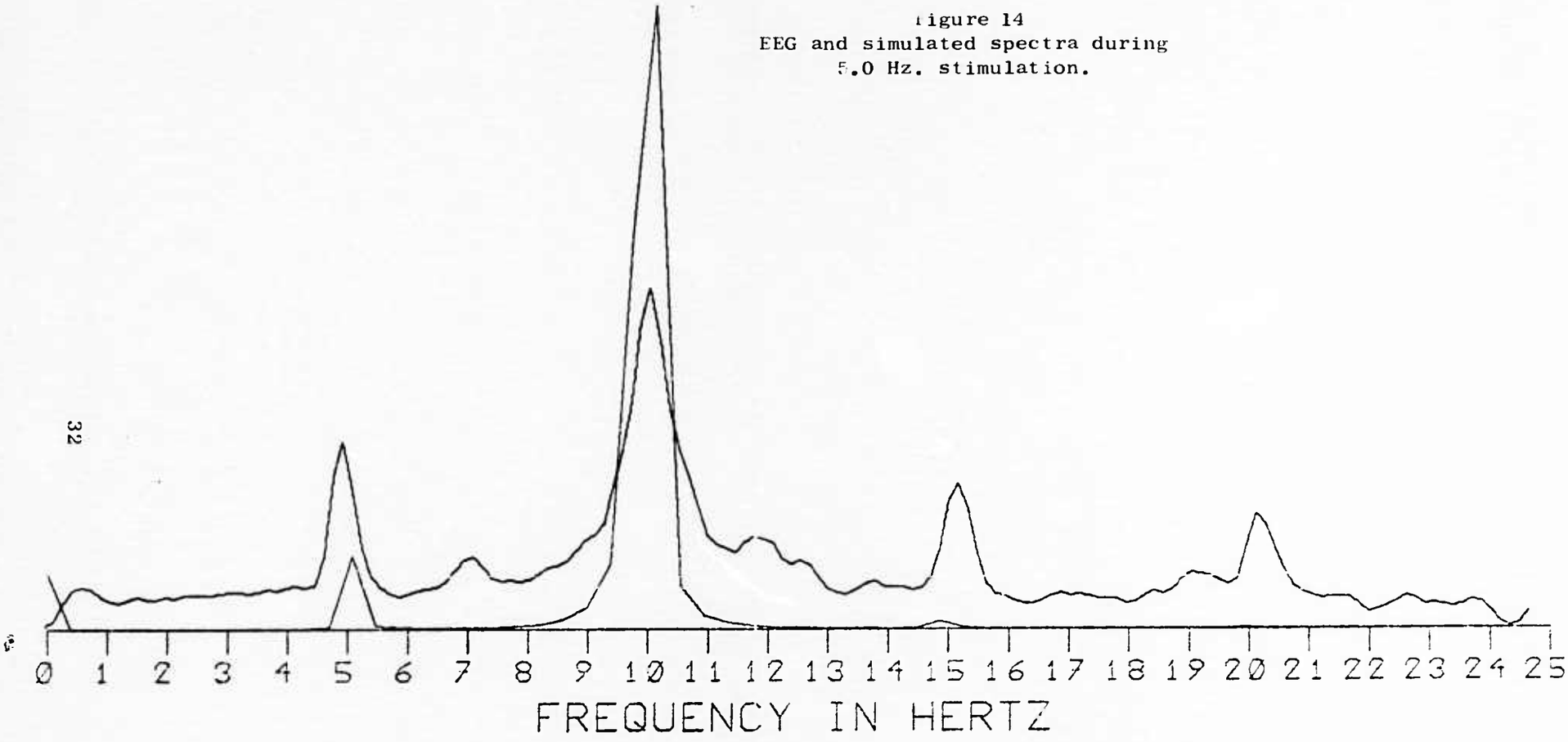

Figure 15
EEG and simulated spectra during
19.0 Hz. stimulation.

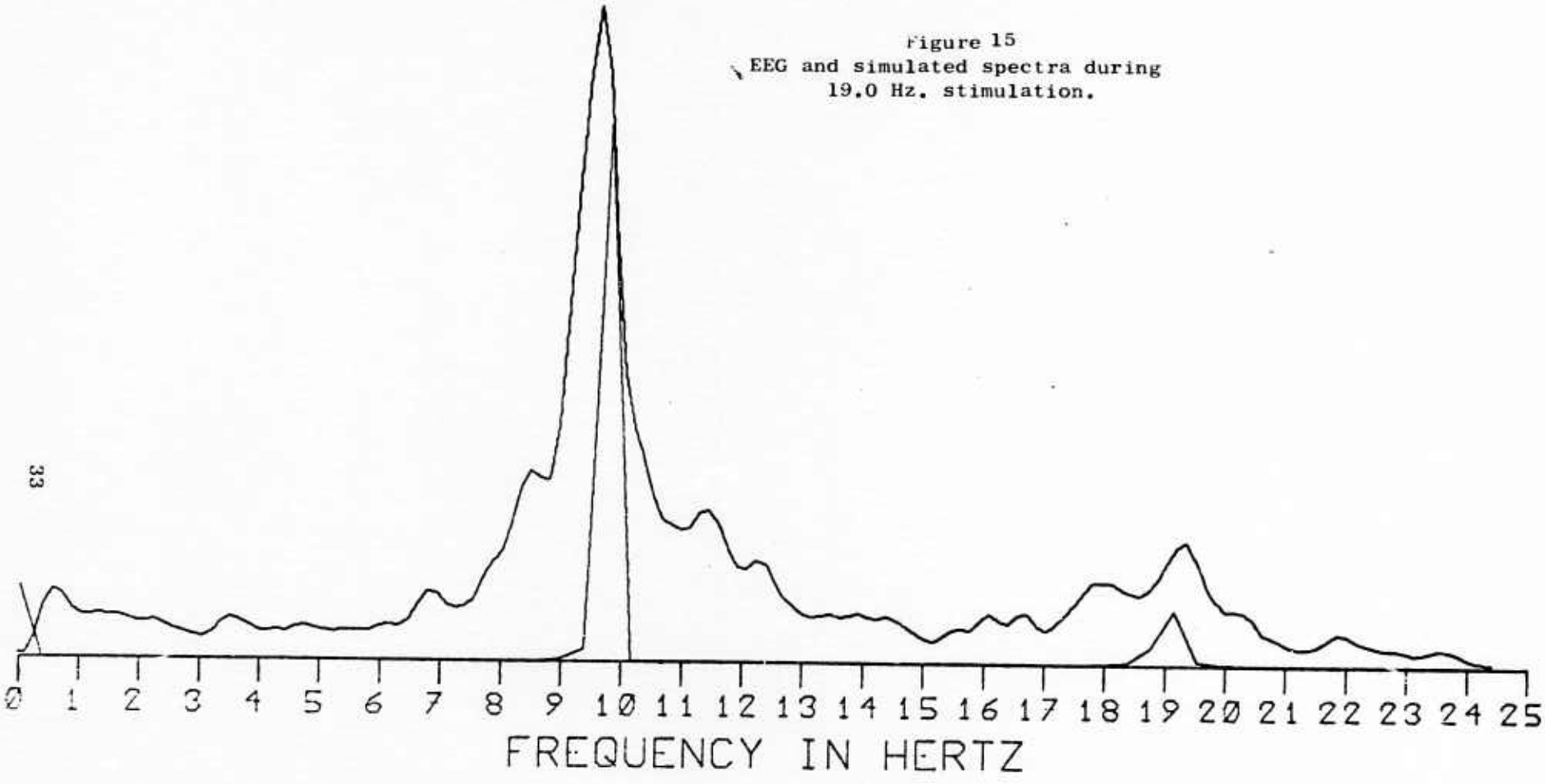

STIMULUS FREQUENCY = 19.00
COUPLING COEFFICIENT = .20000

Figure 16
EEG and simulated spectra during
8.5 Hz. stimulation.

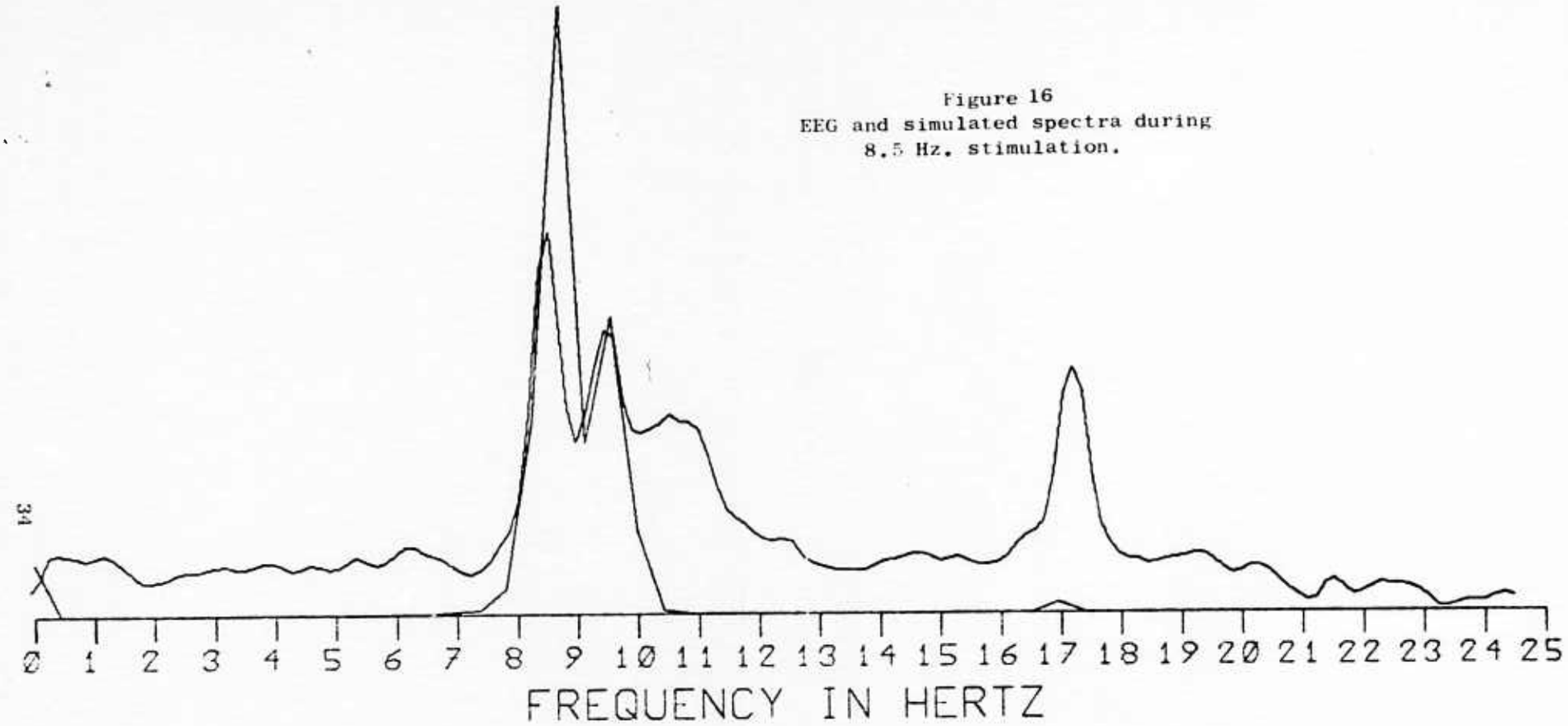

STIMULUS FREQUENCY = 8.50
COUPLING COEFFICIENT = .20000

Figure 17
EEG and simulated spectra during
11.0 Hz. stimulation.

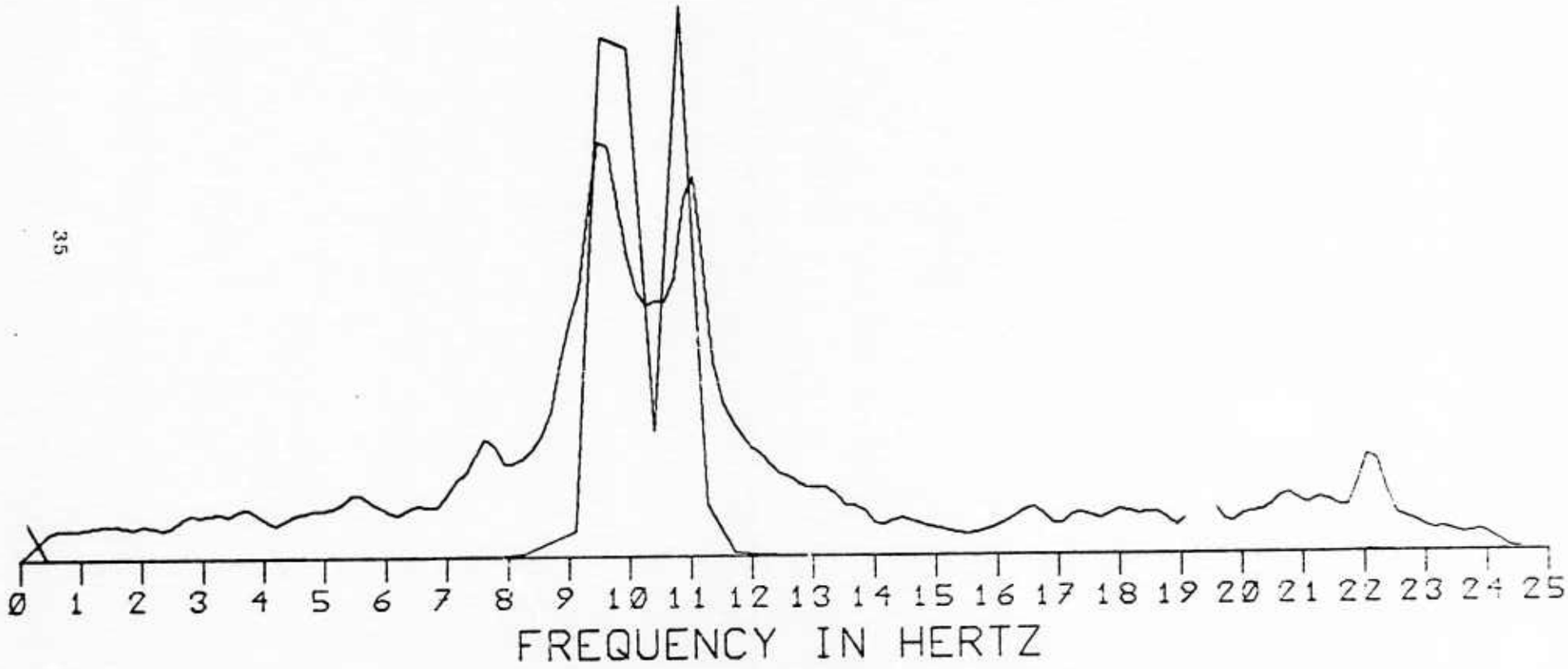

STIMULUS FREQUENCY = 11.00
COUPLING COEFFICIENT = .20000

Figure 18
EEG and simulated spectra during
4.0 Hz. stimulation.

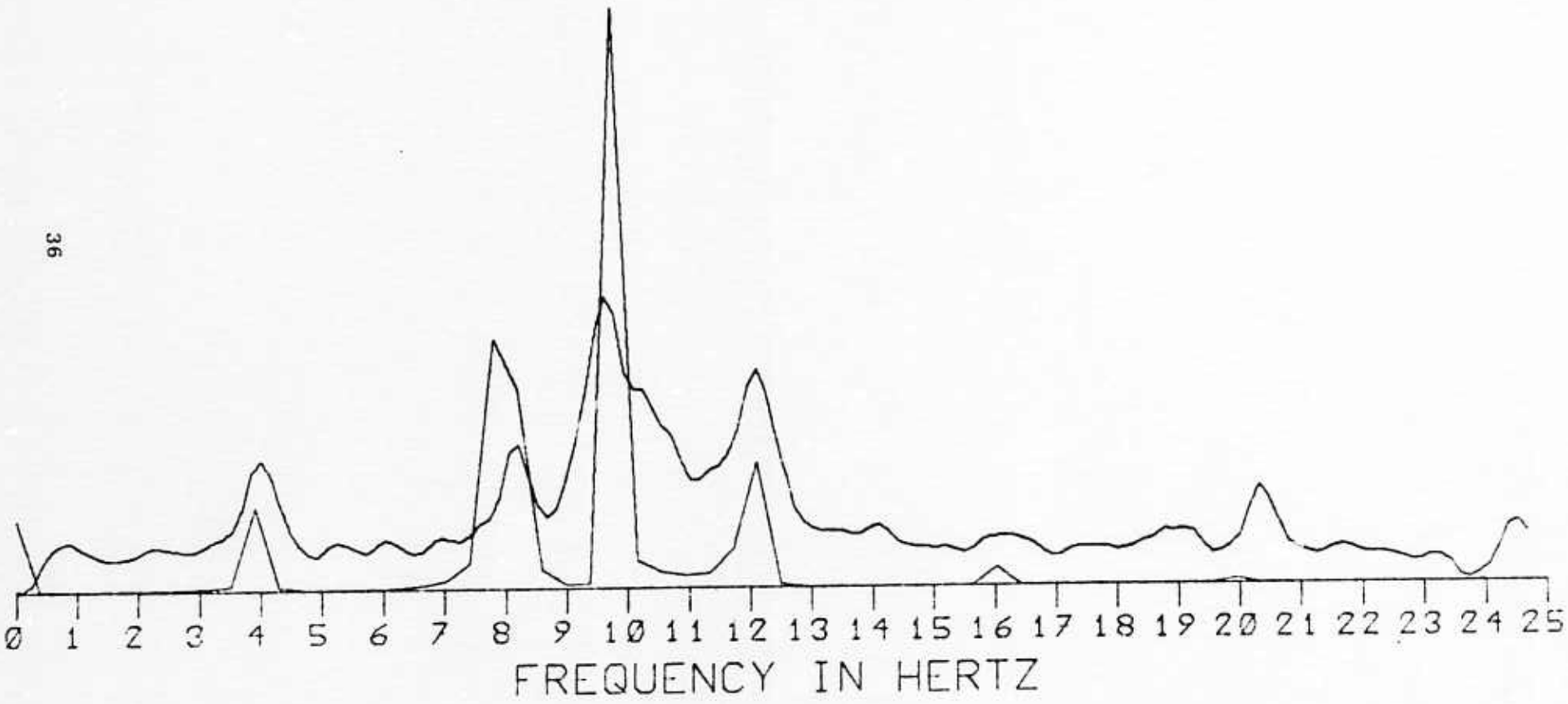

Figure 19
EEG and simulated spectra during
0.5 Hz. stimulation.

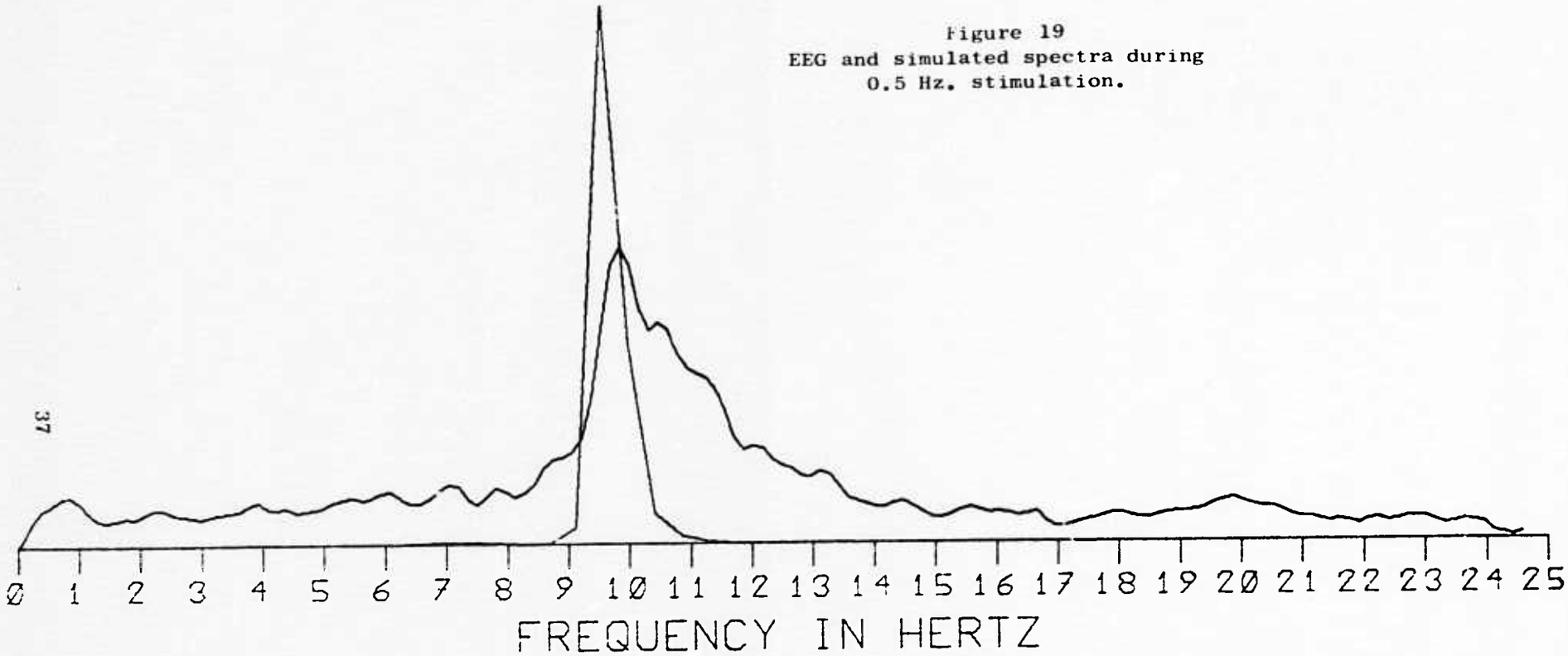

V. GRAF/PEN SYSTEM FOR GENERATING VISUAL STIMULUS PATTERNS

As our work progresses, the need for the capability to generate a variety of visual stimulus patterns in a convenient way increases. The GRAF/PEN system enhances precisely this needed capability.

The GRAF/PEN digitizer (Science Accessories Corporation Model GP-2) consists of a spark pen, writing tablet, an orthogonal set of strip microphones, and electronic accessories. Figure 20 shows the hardware of this system. The X and Y coordinates of the pen are derived from

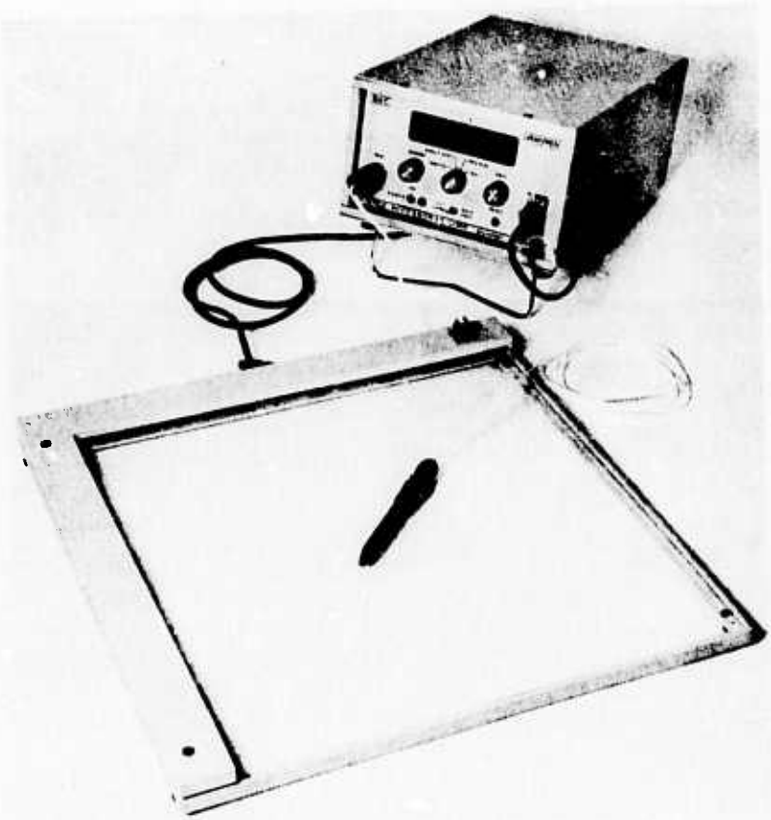

Figure 20 GRAF/PEN unit with spark pen, writing tablet, strip microphones, and electronic accessories.

the flight travel times of the sound of sparks initiated at the pen tip. The electric voltages thus generated are fed to the PDP-11 through an inter-

face. The unichannel operating system for the PDP-11 called PIREX has been slightly modified to respond and read the coordinates from the interface and load them into designated locations in core. An event variable is then set in a manner consistent with the overall RSX-III operating system. Each spark whether automatic or manually generated, initiates this process.

A program dubbed "DRAW" has been developed and implemented for the purpose of utilizing the GRAF/PEN digitizer to generate visual stimulus patterns more conveniently for various experiments. By employing two subroutines, the "DRAW" program constructs a file which consists of various picture segments made up of groups of points. Various commands such as DRAW, ERASE, LOCATE, DISPLAY, SCALE, and END have been designed for the user to create and manipulate these files.

The basic data structure consists of picture segments as shown in Figure 21. The -999 indicates the beginning of a segment. The header length word indicates the length of the header to follow. This header is meant to hold information for classifying the succeeding picture segment in such a way that selective retrieval and display can be easily performed. The header was designed to be of variable length so as to allow for future enhancements. The end of a picture file is signified by -111.

The "DRAW" software is designed as a man-machine interactive program. When the program DRAW is first requested, it asks for a picture file name. The user's replay will prompt the machine to ask whether the user wishes to append picture segments to an old file by this name. If the user does not wish to append, then a new file will be created. The program will then wait for picture commands. The user's commands are

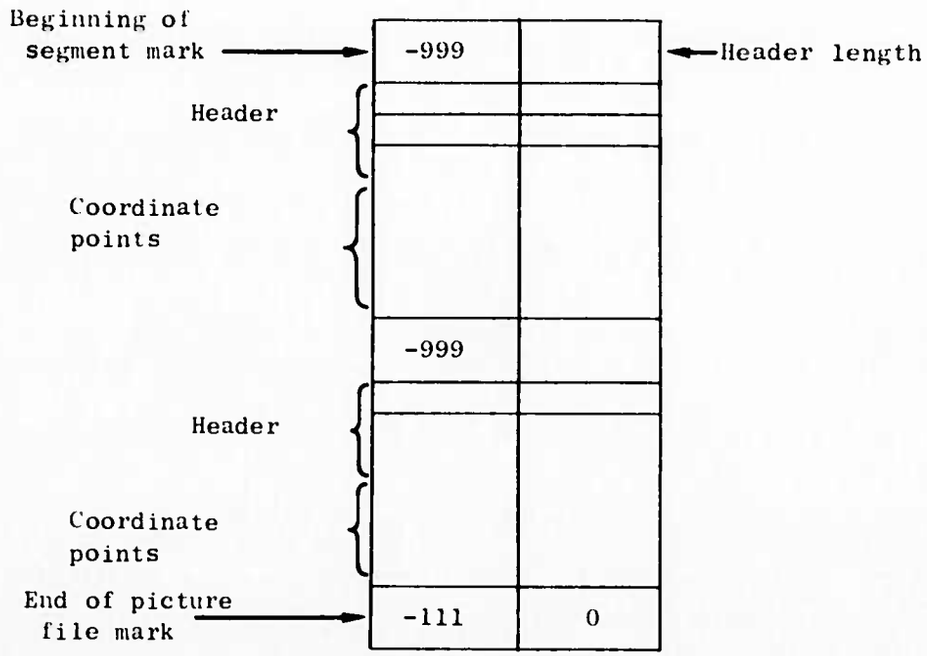

Figure 21 Data structure for picture segments and files.

entered via a menu-type scheme using the GRAF/PEN tablet. The lower right hand corner of the writing tablet is designated as the command section. Particular areas in this section correspond to various commands. The function of each command is described as follows:

"LOCATE" is a command which will map points on the GRAF/PEN tablet to corresponding points on a 611 Tektronics oscilloscope display. This allows the user to locate the picture points already on the display in relation to the pen location on the tablet.

The "DRAW" command constructs a picture segment. It first enters a -999 which indicates the beginning of a segment and then the header length. Any previously entered header information will then be inserted. Successive point are read from the GRAF/PEN until another command is encountered. These data points are analyzed spatially as they are

enetered into the file. Points within a certain distance of each other are discarded so as to prevent bunching and wasteful redundant information. An operation similar to LOCATE is used to display the points that are stored on the 611 scope. This enables the user to monitor the progress of his drawing.

"DISPLAY" will cause the display of all the picture segments which have previously been generated. It automatically extrapolates between successive points in a segment. The displayed picture can be plotted on either the 611 storage scope or CalComp plotter. Figures 22 and 23 show such an example.

"ERASE" will cause the deletion of either the last twenty points or up to the previous picture segment, which ever occurs first. It also crosses out the points which have been erased on the 611 scope so as to allow the user to examine what portion has been actually erased. An example is shown in Figure 24.

"SCALE" will determine the mapping from the GRAF/PEN tablet (4096 × 4096 raster units) to the 611 scope or CalComp plotter (1023 × 1023 raster units). Most linear mappings such as horizontal and vertical gain, rotation, horizontal and vertical offset, and skew can be handled with ease. The coordinate space of the mapping is defined by three points; viz., the endpoint of the Y axis, the origin, and the endpoint of the X axis. This mapping is performed whenever "DRAW", "ERASE", "LOCATE", and "DISPLAY" were actuated.

The "END" command will close the picture file and transform it into a disk file. The system is also reset by this command.

The "DRAW" program can presently handle picture files of up to 128,000 points partitioned in any number of segments. A primitive

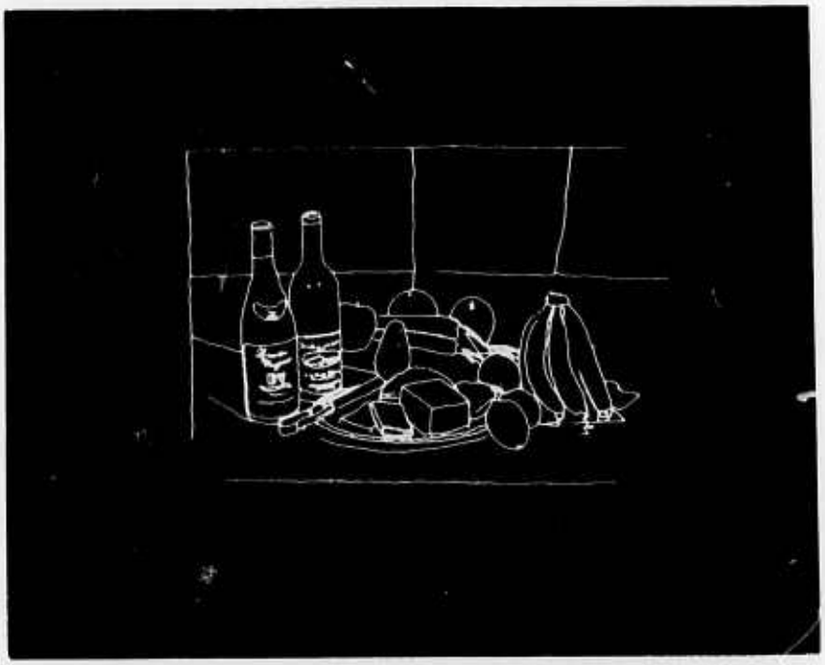

Figure 22 Typical picture produced by the GRAF/PEN as displayed on the 611 display scope.

Figure 23 Picture as displayed on a CalComp.

Figure 24 Picture has been partially erased and displayed with a different scale.

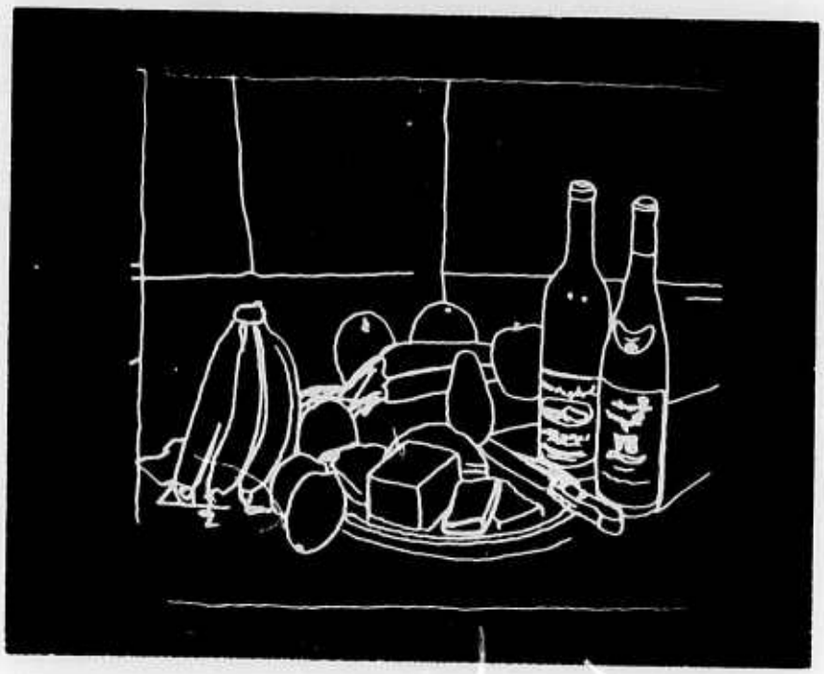

Figure 25 Picture has been inverted and scaled in a different manner.

virtual memory mechanism was implemented to handle efficiently such large files. The actual program was written in a modular form so that any future modifications and expansion can be done with the least effort. The "DRAW" software has greatly enhanced our capability to produce pictorial stimulus patterns.

We have also modified the "SEER" program, which was designed for visual scanpath study. The program enables us to analyze the scanpath in the domain of the "distorted" picture; i.e., the recorded data from the eye-movement monitor as a subject views a "SEER" picture. In order to have the distorted picture correspond more closely to the original picture, a routine has been added to the "DRAW" software which allows simple scaling and offsetting of the response data so that the size and placement of the distorted picture more closely approximates the original stimulus pattern. The only distortion then remaining is the result of nonlinearities in the eye-movement monitor and noise in the system. As a result, feature identification and the location of the subject's visual attention on the picture may be made in the distorted picture domain.

The "ADJUST" routine draws the current picture on both the main and remote 611 scopes, then digitizes EMM location data and displays a "+" on the main 611 scope screen corresponding to the location of the subject's visual attention. By adjustment of two sets of scaling and offset amplifiers (one set for each of the X and Y directions), as the subject looks from point to point at the drawn picture, the response data may be adjusted to correspond in size and location to the stimulus picture. When the program exits, scaling and offset constants are computed which allow the operator to return to the

raw data form if desired

In addition, in the VIEW mode of operation, the response data is displayed on the main 611 scope as the subject views the picture on the remote scope. Thus, the operator may determine if the adjustment is sufficiently accurate for the analysis to be done.

The problem of visual overshoot on the part of the subject, when an abrupt change of direction occurs in the stimulus picture, has been minimized by the addition of a "slow down" routine for the VIEW mode of operation. A SEER picture file is prepared for this application by the program SPEED which inserts a delay count at the location of a change in direction of the picture. The amount of delay and the threshold magnitude for the change of direction is determined by operator responses to questions on the VTØ5. Thus, the speed at which the picture is drawn slows down at the areas of rapid change in direction, and the subject has less of a tendency to overshoot that change in direction.

As an improvement in the speed at which SEER responds to commands to fetch and store picture files, all picture files are now stored in their binary rather than symbolic form; additionally, less storage space is required on the disk for pictures in their binary form.

VI. CONCLUSION

Our work has been progressing along the lines as proposed. As reported, we have developed models for saddadic eye movements and EEG signals with the aim of developing better techniques for tracking and prediction of eye positions and cortical states. With the continuously up-dated information concerning the eye position and cortical state for adjusting the stimulus parameters and the tracking and prediction techniques, we will then be able to guide the eyes to fixate at optimal locations and at optimal time instants such that the vividness and persistence of the desired after-image is enhanced. Hopefully, the EEG model will also provide a better assessment of its role as a timing mechanism in processing visual information. This, in turn, will aid us in determining these optimal time instants. The study of visual scanpaths for the purpose of differentiating scanpaths associated with superior memory from those associated with ordinary memory will give us a firmer grip in the establishment of optimal locations for the eyes to fixate and the optimal scanning sequence for the eyes. For this purpose, a better grip and consistent characterization of visual scanpaths are necessary. To this end, we have developed statistical means for the characterization of visual scanpaths. We have also developed and implemented a man-machine interactive system for generating visual stimulus patterns. Our immediate task is to determine those optimal locations and optimal time instants mentioned previously. Using this information, we shall attempt to devise real-time strategies for the control of visual pattern impression and visual image (memory) persistence and/or recall ability to close the feedback loop in our design

of the closely-coupled man-machine system for visual memory tracking and training.

In this report and also in various conference papers, we have presented our accomplishments and results to date. Further works as outlined are in progress.

REFERENCES

[1] Hyde, J. E., "Some Characterisitics of Voluntary Human Ocular Movements in the Horizontal Plane", Amer. Journal of Ophthal., 1959, 48, 85-94.

[2] Westheimer, G., "Mechanism of Saccadic Eye Movements", Arch. Ophthal., 1954, 52, 710-724.

[3] Yarbus, A. L., Eye Movements and Vision, New York: Plenum Press, 1967.

[4] Young, L. R., Forster, J. D., and Van Houtte, N., "A Revised Stochastic Sampled Data Model for Eye-Tracking Movements", Fourth Annual NASA-Univ. Conference on Manual Control, University of Michigan, Ann Arbor, Michigan, 1968.

[5] Robinson, D. A., "Progress in Models of Eye-Movement Control", Proc. Int'l Conference on Cybernetics and Society, 1972, 14-24.

[6] Robinson, D. A., "Models of the Saccadic Eye-Movement Control System", Kybernetic, 1973, 14, 71-83.

[7] Noton, D., "A Theory of Visual Pattern Perception", IEEE Trans. on Systems Science and Cybernetics, Oct. 1970, SSC-6, 4, 349-357.

[8] Noton, D., and Stark, L., "Scanpaths in Saccadic Eye Movements While Viewing and Recognizing Patterns", Vision Research, 1971, 11, 929-942.

[9] Duda, R. O. and Hart, P. E., Pattern Classification and Scene Analysis, New York: J. Wiley, 1973, p. 203.

[10] Page, R. L., Algorithm 479, Collected Algorithms of the ACM.

LIST OF PUBLICATIONS

[1] A. Shah and D. C. Lai, "Computer Determination of Eye Fixations and Saccades", presented at the 27th Annual Conference on Engineering in Medicine and Biology, Philadelphia, Penn., October 6-10, 1974, and published in the Proceedings, p. 103.

[2] J. R. Nickolls, D. C. Lai, and J. E. Anliker, "A Nonlinear Model of EEG Entrainment by Periodic Photic Stimulation", presented at the Seventh Annual Conference of the Neuroelectric Society, New Orleans, La., November 20-23, 1974, and published in the Proceedings, pp. 13-14.

[3] H. S. Magnuski, "Remark on Algorithm 479[z]", has been accepted for publication in the December issue of Communications of the Association for Computing Machinery.

[4] A. Shah, D. C. Lai, and J. E. Anliker, "Prediction of EEG Waveforms by Using Autoregressive Model", has been accepted for presentation at the 1975 San Diego Biomedical Symposium and scheduled for publication in its Proceedings.

[5] D. C. Lai, J. E. Anliker, and R. V. Floyd, "The Effect of Photic Stimulation in Human EEG Signals", submitted to IEEE for publication.